J. Mol. Biol. (1986) **191**, 553–561

Solution Structure of Human Growth Hormone Releasing Factor

Combined Use of Circular Dichroism and Nuclear Magnetic Resonance Spectroscopy

G. Marius Clore[1], Steven R. Martin[2] and Angela M. Gronenborn[1]

[1]*Max-Planck-Institut für Biochemie D-8033 Martinsried bei Munchen, F.R.G.*

[2]*Division of Physical Biochemistry National Institute for Medical Research Mill Hill, London NW7 1AA, U.K.*

(Received 3 March 1986, and in revised form 20 June 1986)

The solution structures of two human growth hormone releasing factor analogues, ^{27}Leu^{45}Gly-hGHRF(1–45)OH and ^{27}Nle-hGHRF(1–29)NH_2, are investigated by means of circular dichroism and nuclear magnetic resonance spectroscopy. Using circular dichroism spectroscopy, it is shown that both peptides adopt ordered structures at low concentrations of trifluoroethanol (~30%). Quantitative analysis of the circular dichroism spectra indicates that the same number of residues, approximately 23 to 25, are in a helical state in both peptides. Using two-dimensional nuclear magnetic resonance methods all proton resonances of the ^{27}Nle-hGHRF(1–29)NH_2 fragment are assigned and its secondary structure is determined from a qualitative interpretation of the nuclear Overhauser enhancement data. Two distinctive regions of α-helix are present extending from residues 6 to 13 and 16 to 29.

1. Introduction

Growth hormone releasing factor is a 44-residue amidated peptide that stimulates the secretion of growth hormone *in vivo* of all vertebrate species studied to date (Ling *et al.*, 1985). Clinical studies on human growth hormone releasing factor (hGHRF)† are under way and it appears that hGHRF and related analogues may prove to be the most physiological and the cheapest replacement therapy for many growth hormone deficient patients (Noon & Brook, 1985). Physiological studies have shown that the active core of the molecule resides in the N-terminal region and that the hGHRF(1–29) amide fragment retains almost complete biological activity relative to longer sequences both *in vivo* and *in vitro* (Lance *et al.*, 1984). Despite the considerable physiological and clinical interest in hGHRF, nothing is known about its structure in solution.

In this paper we present a combined c.d. and n.m.r. study on the solution structure of two hGHRF analogues, namely ^{27}Leu^{45}Gly-hGHRF(1–45)OH and ^{27}Nle-hGHRF(1–29)NH_2. In both analogues the methionine residue at position 27 is replaced by another hydrophobic residue, Leu and Nle, respectively, an alteration that has no effect on biological activity (W. Wetekam, personal communication). We show that, although neither peptide has an ordered structure in water alone, an ordered structure is induced by low concentrations of trifluoroethanol (TFE) in aqueous solution. From the c.d. data it is shown that the number of helical residues induced by TFE is the same for both molecules, indicating that all the helical regions in the ^{27}Leu^{45}Gly-hGHRF(1–45)OH peptide occur in the first 29 residues. Using two-dimensional n.m.r. methods, the ^{1}H n.m.r. spectrum of the ^{27}Nle-hGHRF(1–29)NH_2 fragment is completely assigned and its secondary structure deduced from a

† Abbreviations used: hGHRF, human growth hormone releasing factor; c.d., circular dichroism; n.m.r., nuclear magnetic resonance; TFE, trifluoroethanol; NOE, nuclear Overhauser enhancement; NOESY, two-dimensional NOE spectroscopy; p.p.m., parts per million.

0022–2836/86/190553–09 $03.00/0

qualitative interpretation of the nuclear Overhauser enhancement (NOE) data.

2. Methods

^{27}Leu^{45}Gly-hGHRF(1–45)OH and ^{27}Nle-hGHRF(1–29)NH_2 were gifts from Drs W. Wetekam and H. Müllner (Hoechst) and Dr F. Momany (Polygen), respectively. Both peptides were >99% pure as judged by high-pressure liquid chromatography.

Samples for c.d. spectroscopy contained 0·15 mg peptide/ml in 20 mM-sodium acetate buffer (pH 4·0) and varying amounts of TFE. For the n.m.r. measurements 2 samples of the (1–29) peptide were prepared: each contained 4 mM-peptide in 20 mM-phosphate buffer (pH 4·0) and 30% (v/v) d_3-TFE; in addition one contained 70% ^2H_2O and the other 63% H_2O and 7% ^2H_2O. All c.d. and n.m.r. experiments were carried out at 25°C.

c.d. spectra were recorded from 260 to 190 nm on a JASCO J41C spectropolarimeter equipped with a model J-DPY data processor, at sensitivities in the range 0·5 to 5·0 mdeg./cm and with an instrumental time constant of 4 s. Cells with a 1 mm pathlength were used and the spectra are the averages of at least 4 scans. Digitized spectra collected by the data processor were transferred to a PDP 11/23 computer and subsequently processed for base-line subtraction, normalization and smoothing according to the methods of Savitzky & Golay (1964). All spectra are presented as molar circular dichroism, $\Delta\varepsilon$, based upon a mean residue weight of 133·5 (45-mer) or 115 (29-mer). Molar ellipticity can be obtained from the equation $[\theta]_{m.r.w.} = 3300 \times \Delta\varepsilon$. Structure prediction from c.d. spectra were obtained using the CONTIN program of Provencher & Glockner (1981).

All n.m.r. experiments were recorded on a Bruker AM500 spectrometer equipped with digital phase shifters and an ASPECT 3000 computer. For measurements in H_2O the solvent resonance was suppressed by selective irradiation during the relaxation delay, and in the case of the NOESY spectra, during the mixing time as well. All 2-dimensional n.m.r. spectra were recorded with sweep widths of 6024 Hz and the carrier placed approximately in the middle of the spectrum. The digital resolution was 5·88 Hz per point in both dimensions, and this was achieved by appropriate zero-filling in the t_1 dimension only. In all cases the 2-dimensional spectra were symmetrized (Bauman *et al.*, 1981). The 2-dimensional spectra were recorded in the pure-phase absorption mode using the time proportional-phase incrementation method (Redfield & Kuntz, 1975; Bodenhausen *et al.*, 1980) as described by Marion & Wuthrich (1983). Homonuclear Hartmann-Hahn MLEV17 spectra (Davies & Bax, 1985; Bax & Davies, 1985), a variant of coherence transfer spectroscopy by isotropic mixing (Braunschweiler & Ernst, 1985), were recorded at 4 mixing times (15, 25, 60 and 87 ms) corresponding to direct, single and multiple relayed through-bond magnetization transfers. NOESY spectra (Jeener *et al.*, 1979; Macura *et al.*, 1981) were recorded at 3 mixing times (100, 200 and 300 ms). In both cases, appropriate phase cycling was used for the suppression of axial peaks. In the case of the NOESY spectra, additional phase cycling was also used to suppress cross-peaks due to multiple quantum coherence transfer, and a 10% random variation in the mixing time was used to eliminate zero quantum coherence transfer. Typically 64 to 128 transients were collected for each of 600 increments with a relaxation delay of 1 s between successive transients. An initial phase correction was carried out during transformation with a final adjustment after completion of the 2-dimensional transform.

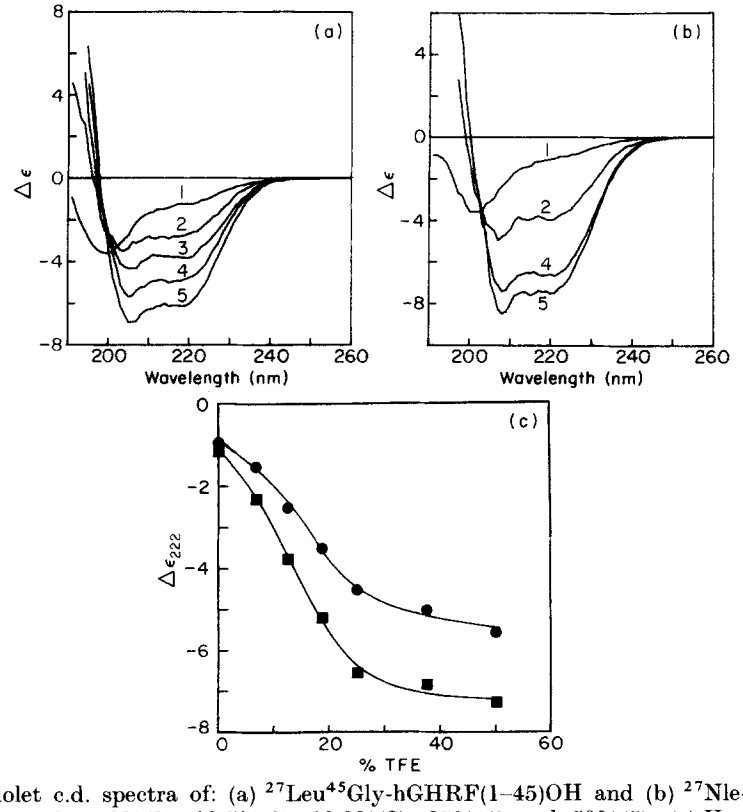

Figure 1. Far ultraviolet c.d. spectra of: (a) ^{27}Leu^{45}Gly-hGHRF(1–45)OH and (b) ^{27}Nle-hGHRF(1–29)NH_2 as a function of TFE concentration: 0%(1), 12·5%(2), 18·8%(3), 25%(4) and 50%(5). (c) Variation of molar circular dichroism at 222 nm as a function of TFE concentration (●, 1–45 peptide; ■, 1–29 peptide).

3. Results and Discussion

(a) *Circular dichroism*

Figure 1(a) shows the far ultraviolet c.d. spectrum of the ^{27}Leu^{45}Gly-hGHRF(1–45)OH peptide aqueous solution (20 mM-acetate buffer at pH 4·0) and in the same buffer containing different amounts of TFE. Qualitatively, the spectrum in aqueous solution is that of a polypeptide with a significant amount of β structure but with only a small helical content. Upon increasing the TFE content of the solution there is a dramatic increase in the helix content as shown, in particular, by the appearance of the distinctive high-intensity negative band at 222 nm. A similar experiment for the ^{27}Nle-hGHRF(1–29)NH_2 fragment is shown in Figure 1(b). The results are essentially identical to those with the whole molecule except that the increase in helix content appears to be more marked and the molar circular dichroism of the fragment is greater than that of the whole molecule. This is easily seen from the variation in the molar circular dichroism at 222 nm as a function of TFE concentration shown in Figure 1(c).

These qualitative observations are confirmed by analysing the c.d. spectra for secondary structure content using the CONTIN program (Provencher & Glockner, 1981) and the results are summarized in Figure 2. In aqueous solution both the whole molecule and the (1–29) fragment have a relatively high beta content (~50%) and very low helix content, as suggested by the c.d. spectra. In the case of the whole molecule the helix content increases from 6% to 56% on going from aqueous buffer to the same buffer containing 50% TFE. Most of the increase appears to come from a loss of β structure, which is reduced from 45% to 16%, with the random (plus reverse turn) structure only dropping from 47% to 28%. The situation with the (1–29) fragment is very similar. On going from aqueous solution to the solution with 50% TFE the helix content increases from 10% to 81%. As with the whole molecule there is a substantial loss of β structure (56% to 7%) and a smaller change in random (plus reverse turn) structure. Two features of the TFE-induced transition are noteworthy. First, the number of helical residues found for the spectra recorded in 50% TFE is the same within experimental error for both the whole molecule and the (1–29) fragment, and comprises approximately 23 to 25 residues (Fig. 2(a)). This suggests that all the helical segments in the ^{27}Leu^{45}Gly-hGHRF(1–45)OH peptide occur in the first 29 residues. Second, the transition itself is essentially complete at an unusually low (~30%) TFE concentration, indicating that a relatively small perturbation of the solvent conditions, namely a small reduction in the water activity, is all that is required to induce the α-helical structure in hGHRF. This is consistent with the presumed site of action of hGHRF at a membrane-bound pituitary receptor (Ling *et al.*, 1985).

The high value for β content derived from the c.d. analysis of both the ^{27}Nle-hGHRF(1–29)NH_2 and ^{27}Leu^{45}Gly-hGHRF(1–45)OH peptides seems at first a little surprising, particularly as n.m.r. spectroscopy in aqueous solution (in the absence of TFE) shows no sign of an ordered structure for either molecule. Indeed almost no sequential NOEs were observed and there was no evidence for the presence of a β-sheet. Thus, it seems likely that the distribution of β and random coil structure derived from the c.d. spectra simply provides a measure of the average backbone conformation of a peptide in dynamic equilibrium between many states, which not surprisingly exhibits quite a high β content given that the ϕ, ψ backbone torsion angles of a β-strand represent one of the preferred regions of conformational space (Ramachandran & Sasisekharan, 1968). A second point to bear in mind is that the CONTIN analysis is based on data derived from 16 large globular proteins (Provencher & Glockner, 1981). For such large proteins both linear effects, arising, for example, from distortions of regular conformation, and non-linear effects, such as the dependence of mean residue ellipticity on helix length, β-sheet length or β-sheet width, tend to be averaged out over the large number of residues so that they are not very different from one protein to the next. For small polypeptides, however, this is unlikely to be the case, so the relative estimates of secondary structure derived

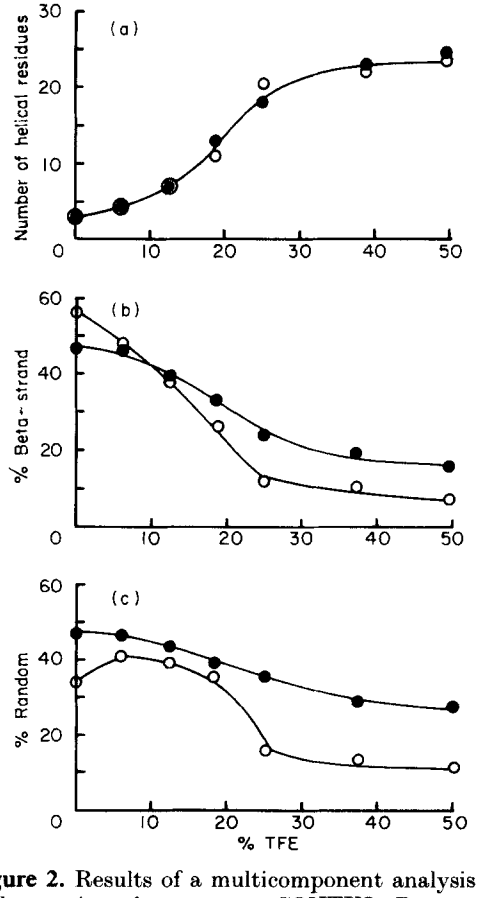

Figure 2. Results of a multicomponent analysis of the c.d. data using the program CONTIN (Provencher & Glochner, 1981) (○, 1–45 peptide; ●, 1–29 peptide).

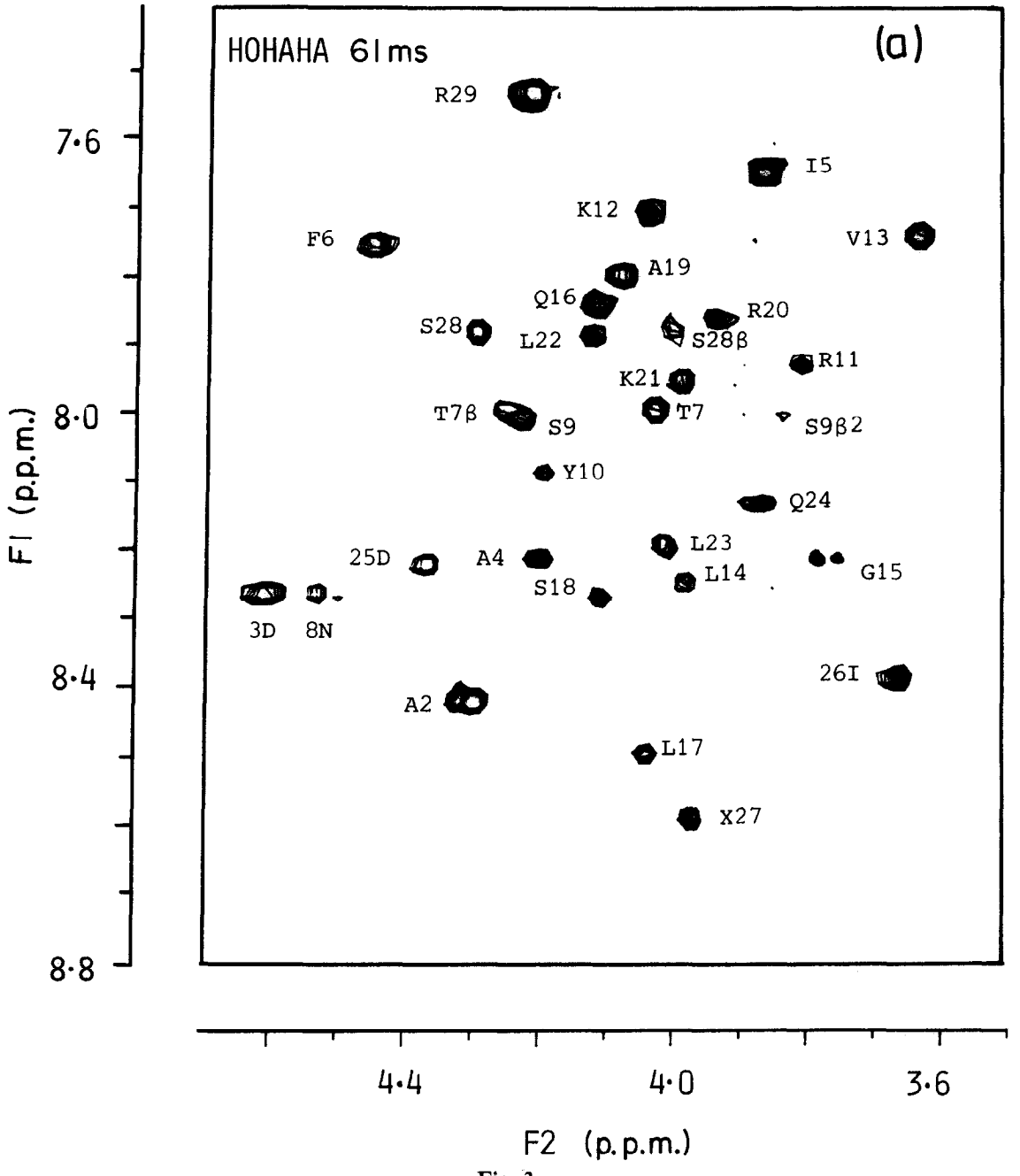

Fig. 3.

from the CONTIN c.d. analysis should only be used as an approximate guide. This is particularly so for the relative contributions of β-strand and random coil structure as the intensity of the random coil c.d. spectrum for peptides is known to be reduced relative to that for proteins (Ziegler & Bush, 1971). Consequently, the percentage β-strand relative to random coil is likely to be overestimated for the two hGHRF polypeptide analogues. With regard to the analysis of α-helix content, however, the contribution of the β-strand and random coil c.d. spectra to the negative 222 nm band of the α-helix spectrum is small so that the estimate of helical content should be reasonably accurate (Chen *et al.*, 1972).

(b) *Assignment of the proton resonances of* ^{27}*Nle-hGHRF(1–29)NH*$_2$

On the basis of the c.d. data, all n.m.r. experiments were carried out in the presence of 30% (v/v) d_3-TFE, a condition ensuring the complete conversion of the ^{27}Nle-hGHRF(1–29)NH_2 fragment to an ordered structure. Lack of sufficient solubility precluded any detailed n.m.r. analysis of the ^{27}Leu^{45}Gly-hGHRF(1–45)OH peptide.

Sequence-specific resonance assignments were carried out in a sequential manner by means of two-dimensional n.m.r. methods (Wüthrich *et al.*, 1982; Wüthrich, 1983; Wagner & Wüthrich, 1982; Štrop

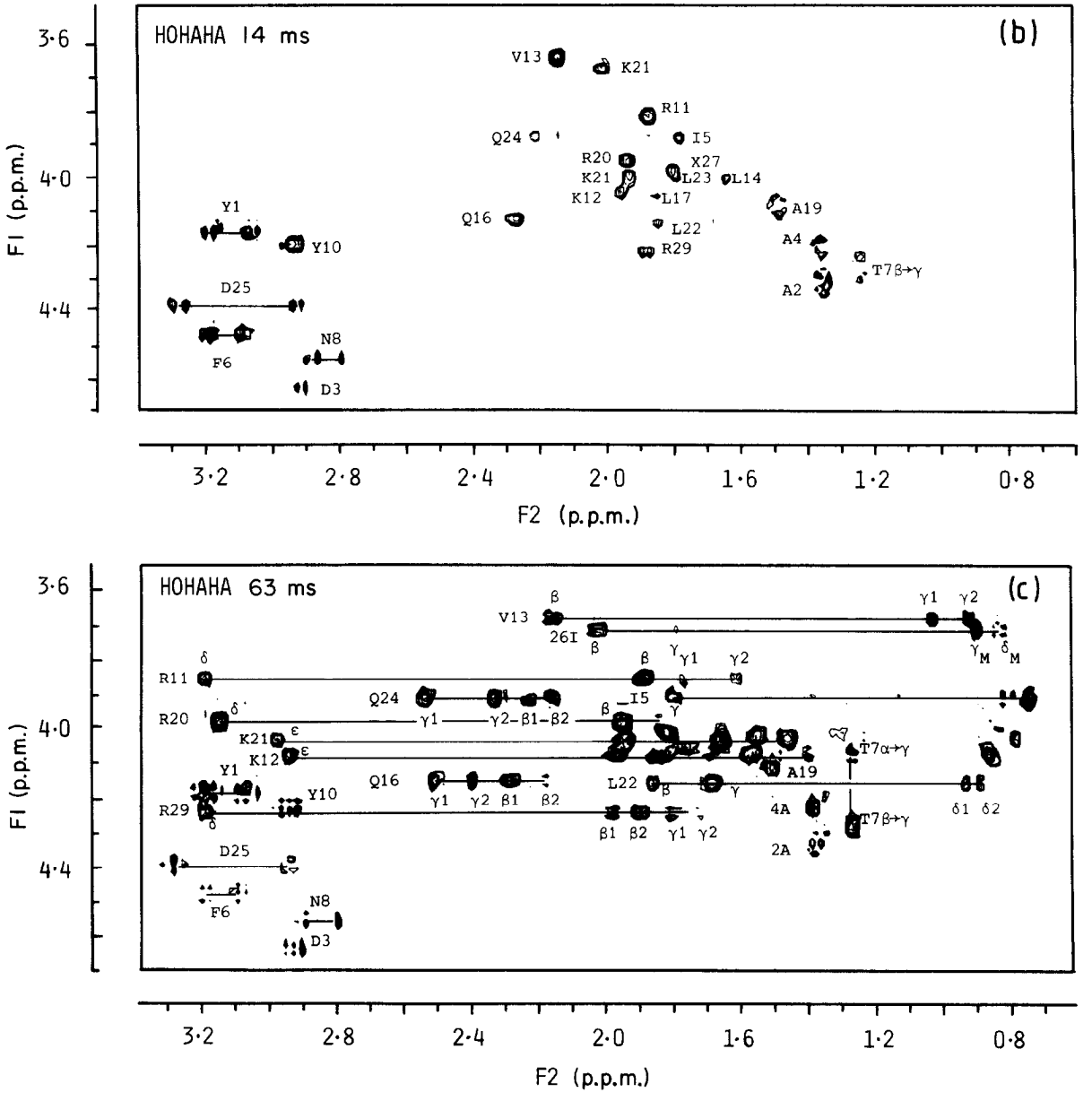

Figure 3. (a) NH(F1 axis)–C$^{\alpha}$H(F2 axis), and (b) and (c) C$^{\alpha}$H(F1 axis)–aliphatic(F2 axis) regions of the pure-phase absorption Hartmann-Hahn spectra of the ^{27}Nle-hGHRF(1–29)NH$_2$ fragment in 30% (v/v) TFE displaying direct and relayed through-bond connectivities. In (a) direct NH–C$^{\alpha}$H connectivities as well as relayed NH–C$^{\beta}$H connectivities involving Ser9, Thr7 and Ser28 are observed; in (b) only direct C$^{\alpha}$H–C$^{\beta}$H connectivities are seen; and in (c) direct and multiple relayed connectivities are seen (e.g. in the case of the 3 arginine residues the entire spin system is apparent). Residues are labelled using the one-letter code and X stands for Nle.

et al., 1983; Zuiderweg *et al.*, 1983). In short, this involves first the identification of amino acid spin systems by means of through-bond connectivities, followed by sequential assignment by means of short (<5 Å) through-space connectivities. All spin systems were identified using Hartmann-Hahn spectroscopy at several mixing times in order to record spectra exhibiting either direct or direct and relayed (single and multiple) through-bond connectivities. Examples of pure-phase absorption Hartmann-Hahn spectra of the NH–C$^{\alpha}$H and aliphatic regions are shown in Figure 3. Through-space connectivities, of which the inter-residue C$^{\alpha}$H(i)–NH($i+1$) (d_1), NH(i)–NH($i+1$) (d_2) and C$^{\beta}$H(i)–NH($i+1$) (d_3) connectivities are the most important for the purpose of sequential resonance assignment, were identified by means of pure-phase absorption NOESY experiments, some examples of which are shown in Figure 4. Particularly useful starting points for the sequential assignment were the two unique amino acid spin systems present in ^{27}Nle-hGHRF(1–29)NH$_2$, namely Thr7 and Val13. In this way we were able to assign the ^{1}H n.m.r. spectrum of the ^{27}Nle-hGHRF(1–29)NH$_2$ fragment completely and unambiguously. The assignment of the proton resonances is given in Table 1.

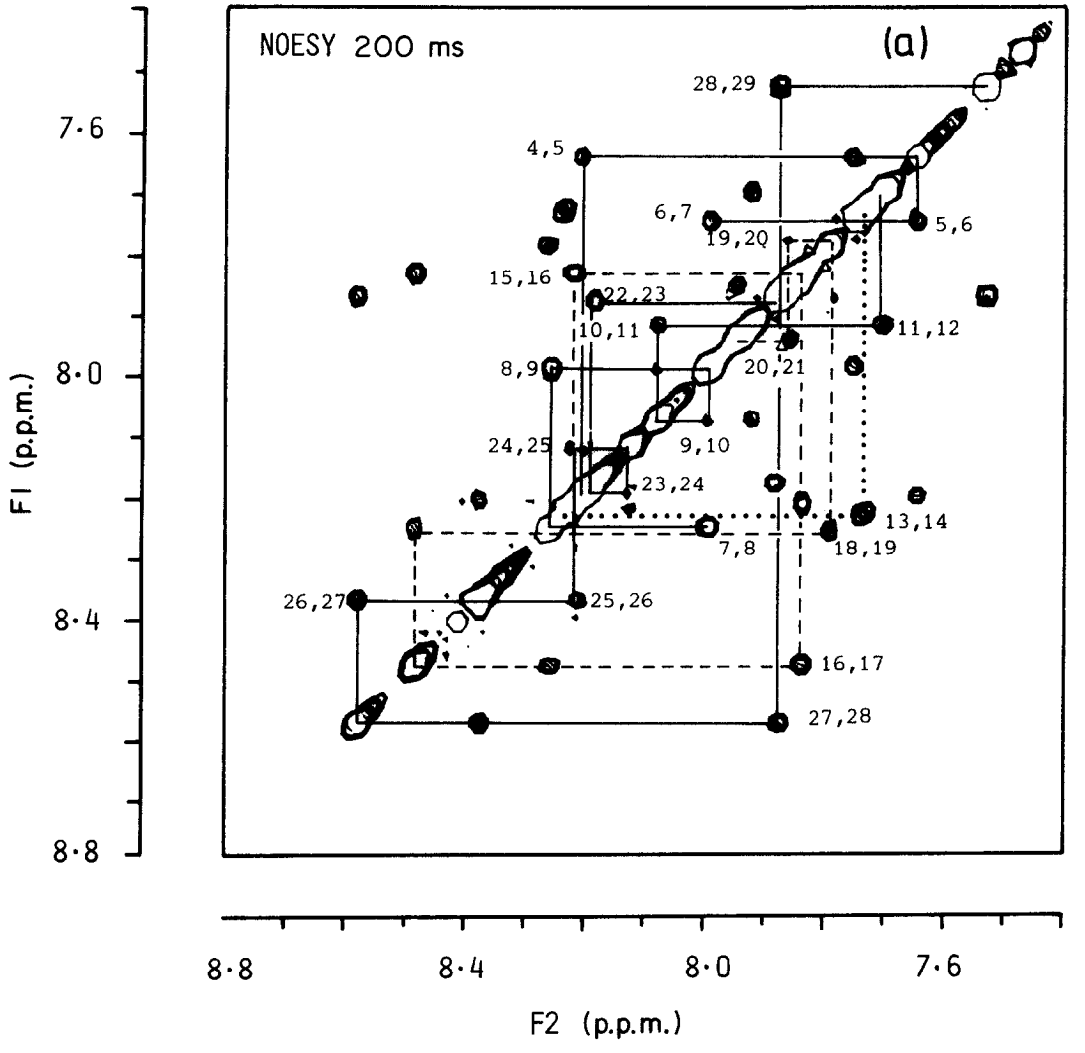

Figure 4. (a) NH(F1 axis)–NH(F2 axis), (b) NH(F1 axis)–$C^{\alpha}H$(F2 axis) and (c) NH(F1 axis)–$C^{\beta}H$/aliphatic(F2 axis) regions of the pure-phase absorption NOESY spectra of the ^{27}Nle-hGHRF(1–29)NH_2 fragment in 30% (v/v) TFE displaying through-space (<5 Å) connectivities. Symbols: (a) NH(i)–NH($i+1$) connectivities from residues 4 to 12 (———), 13 to 14 (·····), 15 to 21 (– – –) and 22 to 29 (———). (b) $C^{\alpha}H(i)$–NH($i+3$) connectivities (———), $C^{\alpha}H(i)$–NH($i+1$) connectivities (– – –) and $C^{\beta}H(i)$–NH(j) connectivities (·····), labelling is at the $C^{\alpha}H(i)$–NH(i) and $C^{\beta}H(i)$–NH(i) cross-peaks.

(c) *Secondary structure of ^{27}Nle-hGHRF(1–29)NH_2 in 30% (v/v) TFE*

From a detailed analysis of the short interproton distances present in various protein secondary structure elements, Wüthrich *et al.* (1984) showed that it is possible to determine the secondary structure of a polypeptide accurately from a qualitative analysis of the NOE data. The quality of the secondary structure obtained in this way has recently been demonstrated convincingly for the α-amylase polypeptide inhibitor from *Streptomyces tendae* where the secondary structure determined by n.m.r. (Kline & Wüthrich, 1985) was found to be in complete agreement with that seen in the crystal structure solved at a later date (Pflugrath *et al.*, 1986). The analysis is based on the following two observations: (1) the NOE cross-peak intensities at short mixing times are approximately proportional to r^{-6} and therefore very sensitive to the value of the interproton distance r; and (2) each secondary structure type has a characteristic set of short interproton distances involving the NH, $C^{\alpha}H$ and $C^{\beta}H$ protons and hence exhibits a characteristic pattern of NOEs. α-Helices are characterized by short NH(i)–NH($i+1$) distances in the range 2·5 to 3 Å, medium-length $C^{\alpha}H(i)$–NH($i+3$) and $C^{\alpha}H$–$C^{\beta}H(i+3)$ distances in the range 3 to 3·5 Å, and $C^{\alpha}H(i)$–NH($i+1$) distances of ~3·5 Å. Extended strands, on the other hand, are characterized by very short $C^{\alpha}H(i)$–NH($i+1$) distances (~2·2 Å) with all other interstrand interproton distances >4 Å (with the exception of the $C^{\beta}H(i)$–NH($i+1$) distances, which show little variation between α-helices and extended strands). In addition to the NOE data, corroborative data can be obtained from two further sources: (1) the $^{3}J_{HN\alpha}$ coupling constants, which are small (<5 Hz) in α-helices,

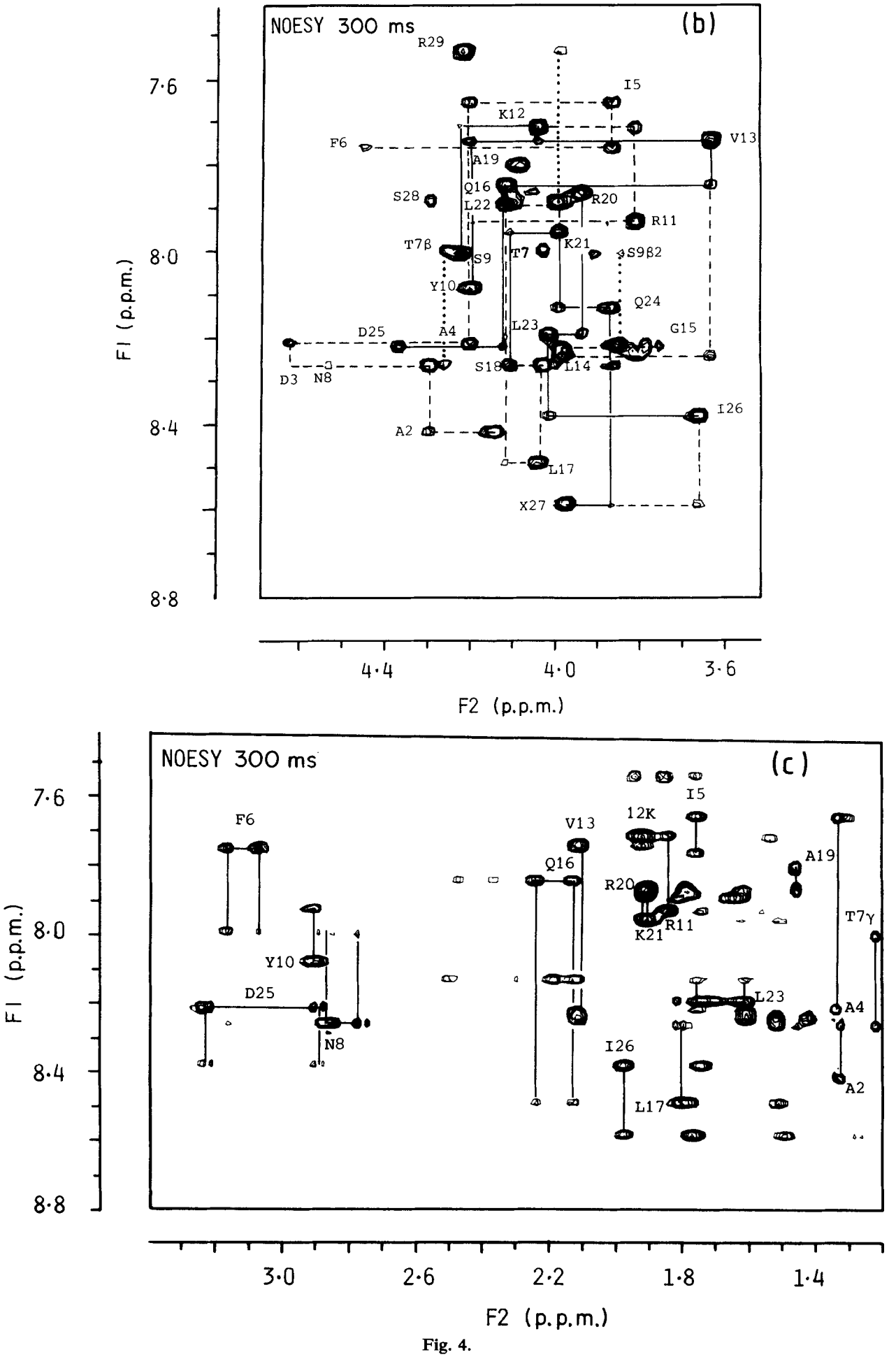
NOESY 300 ms
(b)
R29
I5
K12
F6
V13
A19
Q16
S28
L22
R20
R11
T7β
T7
K21
S9
S9β2
Y10
Q24
D25
A4
L23
G15
D3
N8
S18
L14
I26
A2
L17
X27
7·6
8·0
8·4
8·8
F1 (p.p.m.)
4·4
4·0
3·6
F2 (p.p.m.)
NOESY 300 ms
(c)
F6
I5
12K
V13
Q16
A19
R20
T7γ
K21
R11
Y10
D25
L23
A4
N8
I26
A2
L17
7·6
8·0
8·4
8·8
F1 (p.p.m.)
3·0
2·6
2·2
1·8
1·4
F2 (p.p.m.)

Fig. 4.

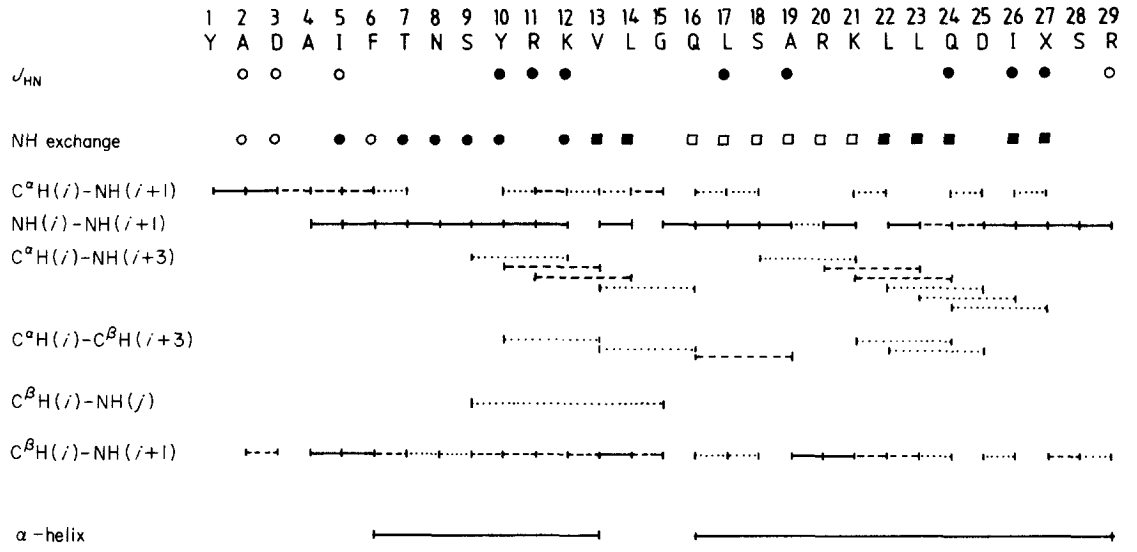

Figure 5. Amino acid sequence of the ^{27}Nle-hGHRF(1–29)NH_2 fragment together with the NOE connectivities involving the NH, $C^{\alpha}H$, $C^{\beta}H$ protons, the $^3J_{HN\alpha}$ coupling constants, the relative amide exchange rates and the secondary structure. The NOEs are classified as follows: (———) strong; (– – –) medium; (· · · · ·) weak. The coupling constant symbols are: (●) $J_{HN\alpha} < 5$ Hz; (○) $J_{HN\alpha} > 7$ Hz. The symbols for the amide exchange rates are: "instant" exchange (○) and exchange after 1 h (●), 12 h (□) and 36 h (■) of taking the sample up in ^2H_2O. The coupling constants were determined from the resolved amide resonances in the one-dimensional n.m.r. spectrum. The apparent peak-to-peak separation of the 2 antiphase components of the cross-peaks in the pure-phase absorption COSY spectra was between 7 and 8 Hz for all NH–$C^{\alpha}H$ cross-peaks so that they could not be used to estimate the $J_{HN\alpha}$ coupling constants as the apparent peak separation tends to a value of ~0·58 times the linewidth at half-height (Neuhaus *et al.*, 1985). In this case the linewidths at half-height are 12 to 14 Hz so that the minimum peak-to-peak separation of the antiphase COSY cross-peaks is 7 to 8 Hz.

Table 1

Assignment of the proton resonances of the ^{27}Nle-hGHRF(1–29)NH_2 fragment in 30% (v/v) TFE at 25°C

Residue	NH	Resonance $C^{\alpha}H$	Resonance $C^{\beta}H$	Others
1 Tyr		4·20	3·20, 3·07	$C^{\delta}H$ 7·16 $C^{\epsilon}H$ 6·87
2 Ala	8·42	4·31	1·37	
3 Asp	8·27	4·63	2·94, 2·90	
4 Ala	8·22	4·21	1·39	
5 Ile	7·67	3·88	1·80	$C^{\gamma}H$ 1·39, 1·12 $C^{\gamma}H_3$ 0·73 $C^{\delta}H_3$ 0·80
6 Phe	7·77	4·46	3·20, 3·09	$C^{\delta}H$ 7·15 $C^{\epsilon}H$ 7·20 $C^{\zeta}H$ 7·24
7 Thr	8·00	4·13	4·30	$C^{\gamma}H_3$ 1·33
8 Asn	8·27	4·53	2·89, 2·79	$N^{\delta}H_2$ 7·50, 6·83
9 Ser	8·02	4·23	3·96, 3·86	
10 Tyr	8·10	4·21	2·96, 2·93	$C^{\delta}H$ 7·00 $C^{\epsilon}H$ 6·75
11 Arg	7·94	3·83	1·89, 1·89	$C^{\gamma}H$ 1·60 $C^{\delta}H$ 3·19 $N^{\epsilon}H$ 7·13
12 Lys	7·73	4·06	1·96	$C^{\gamma}H$ 1·57, 1·40 $C^{\delta}H$ 1·68 $C^{\epsilon}H$ 2·94 NH_3 7·55
13 Val	7·75	3·66	2·15	$C^{\gamma}H_3$ 1·03, 0·91
14 Leu	8·24	4·00	1·66, 1·46	$C^{\gamma}H$ 1·55 $C^{\delta}H_3$ 0·79
15 Gly	8·23	3·81, 3·77		
16 Gln	7·86	4·13	2·28, 2·16	$C^{\gamma}H$ 2·46, 2·37 $C^{\delta}NH_2$ 6·94, 7·23
17 Leu	8·49	4·06	1·86, 1·55	$C^{\gamma}H$ 1·22 $C^{\delta}H_3$ 0·83
18 Ser	8·27	4·12	4·04, 3·90	
19 Ala	7·81	4·09	1·50	
20 Arg	7·88	3·95	1·95, 1·95	$C^{\gamma}H$ 1·83, 1·66 $C^{\delta}H$ 3·15 $N^{\epsilon}H$ 7·20
21 Lys	7·96	4·01	1·94, 1·94	$C^{\gamma}H$ 1·55, 1·47 $C^{\delta}H$ 1·73, 1·65 $C^{\epsilon}H$ 2·96
22 Leu	7·90	4·03	1·76, 1·76	
24 Gln	8·14	3·88	2·21, 2·15	$C^{\gamma}H$ 2·50, 2·29
25 Asp	8·23	4·38	3·20, 2·93	
26 Ile	8·39	3·69	2·02	$C^{\gamma}H$ 1·79, 1·12 $C^{\gamma}H_3$ 0·90 $C^{\delta}H_3$ 0·84
27 Nle	8·59	3·99	1·83	$C^{\gamma}H$ 1·55 $C^{\delta}H$ 1·30, 1·20 $C^{\epsilon}H_3$ 0·83
28 Ser	7·89	4·30	4·03	
29 Arg	7·55	4·22	2·99, 1·89	$C^{\gamma}H$ 1·89, 1·71 $C^{\delta}H$ 3·19 $N^{\epsilon}H$ 7·13

Chemical shifts are in p.p.m. relative to 4,4-dimethylsilapentane-1-sulphonate.

indicative of backbone torsion angles ϕ in the range $-40°$ to $-90°$, and large (>8 Hz) in extended strands, indicative of ϕ in the range -80 to $-160°$ (Pardi *et al.*, 1985); and (2) slow amide-exchange rates indicative of hydrogen bonding (Wagner *et al.*, 1981).

The observed NOEs involving the NH, $C^{\alpha}H$ and $C^{\beta}H$ protons of the ^{27}Nle-hGHRF(1–29)NH_2 fragment, classified as strong, medium and weak, together with the $^3J_{HN\alpha}$ coupling constant and amide exchange data are summarized in Figure 5. These data reveal two distinct α-helical regions: the first extending from residues 6 to 13 and the second from 16 to 29. The region from residues 13 to 16 probably comprises a half-turn based both on the pattern of $C^{\alpha}H(i)$–$NH(i+1)$ and $NH(i)$–$NH(i+1)$ connectivities and on the presence of an NOE between a $C^{\beta}H$ proton of Ser9 and the NH proton of Gly15. Residues 1 to 3 form an extended β-strand and residues 3 to 6 a half-turn.

Apart from the NOE between Ser9 and Gly15, no long-range NOEs, that is to say between protons separated by more than three residues in the sequence, could be detected. This indicates that the ^{27}Nle-hGHRF(1–29)NH_2 fragment does not fold back on itself into a tertiary structure.

4. Concluding Remarks

In this paper we have shown that the first 29 residues of hGHRF can be induced into an ordered mainly helical structure by a low concentration of TFE. Residues 29 to 45, however, do not adopt a helical structure. As TFE achieves its effect by reducing the water activity, it seems likely that the structure of hGHRF in TFE provides a good representation of the structure of hGHRF at a membrane–water interface. It is clear, however, that some details of the structure may be influenced by the properties of the membrane and this will be the subject of future investigations. Studies are now under way to determine the three-dimensional structure of the ^{27}Nle-hGHRF(1–29)NH_2 fragment on the basis of the NOE data using restrained molecular dynamics (Clore *et al.*, 1985, 1986; Kaptein *et al.*, 1985; Nilsson *et al.*, 1986; Brünger *et al.*, 1986).

This work was supported by the Max-Planck Gesellschaft (G.M.C. and A.M.G.). We thank Drs W. Wetekam and H. Müllner (Hoechst, Frankfurt, F.R.G.) and Dr F. Momany (Polygen, Waltham, U.S.A.) for the gifts of ^{27}Leu^{45}Gly-hGHRF(1–45)OH and ^{27}Nle-hGHRF(1–29)NH_2, respectively.

References

Bauman, R., Wider, G., Ernst, R. R. & Wüthrich, K. (1981). *J. Magn. Reson.* **44**, 402–406.

Bax, A. & Davies, D. G. (1985). *J. Magn. Reson.* **65**, 355–360.

Bodenhausen, G., Vold, R. L. & Vold, R. R. (1980). *J. Magn. Reson.* **37**, 93–106.

Braunschweiler, L. & Ernst, R. R. (1983). *J. Magn. Reson.* **53**, 521–528.

Brünger, A. T., Clore, G. M., Gronenborn, A. M. & Karplus, M. (1986). *Proc. Nat. Acad. Sci., U.S.A.* **83**, 3801–3805.

Chen, Y. H., Yang, J. T. & Martinez, H. M. (1972). *Biochemistry*, **11**, 4120–4131.

Clore, G. M., Gronenborn, A. M., Brünger, A. T. & Karplus, M. (1985). *J. Mol. Biol.* **186**, 435–455.

Clore, G. M., Brünger, A. T., Karplus, M. & Gronenborn, A. M. (1986). *J. Mol. Biol.* **191**, 523–551.

Davies, D. G. & Bax, A. (1985). *J. Amer. Chem. Soc.* **107**, 2821–2822.

Jeener, J., Meier, B. H., Bachmann, P. & Ernst, R. R. (1979). *J. Chem. Phys.* **71**, 4546–4553.

Kaptein, R., Zuiderweg, E. R. P., Scheek, R. M., Boelens, R. & van Gunsteren, W. F. (1985). *J. Mol. Biol.* **182**, 179–182.

Kline, A. & Wüthrich, K. (1985). *J. Mol. Biol.* **185**, 503–507.

Lance, V. A., Murphy, W. A., Sueiras-Dias, J. & Coy, D. H. (1984). *Biochem. Biophys. Res. Commun.* **119**, 265–270.

Ling, N., Zeytin, F., Bohlen, P., Esch, F., Brazean, P., Wehrenberg, W. B., Baird, A. & Guillemin, R. (1985). *Annu. Rev. Biochem.* **54**, 403–423.

Macura, S., Huang, Y., Suter, D. & Ernst, R. R. (1981). *J. Magn. Reson.* **43**, 259–281.

Marion, D. & Wüthrich, K. (1983). *Biochem. Biophys. Res. Commun.* **113**, 967–974.

Neuhaus, D., Wagner, G., Vasnk, M., Kagi, J. H. R. & Wüthrich, K. (1985). *Eur. J. Biochem.* **151**, 257–273.

Nilsson, L., Clore, G. M., Gronenborn, A. M., Brünger, A. T. & Karplus, M. (1986). *J. Mol. Biol.* **188**, 455–475.

Noon, C. & Brook, C. G. D. (1985). *Hospital Update*, **11**, 667–678.

Pardi, A., Billeter, M. & Wüthrich, K. (1984). *J. Mol. Biol.* **180**, 741–751.

Pflugrath, J. W., Wiegand, G., Huber, R. & Vertesy, L. (1986). *J. Mol. Biol.* **189**, 383–386.

Provencher, S. W. & Glockner, J. (1981). *Biochemistry*, **20**, 33–37.

Ramachandran, G. N. & Sasisekharan, V. (1968). *Advan. Protein Chem.* **23**, 283–437.

Redfield, A. G. & Kuntz, S. D. (1975). *J. Magn. Reson.* **19**, 250–254.

Savitzky, A. & Golay, M. J. E. (1964). *Anal. Chem.* **36**, 1627–1639.

Štrop, P., Wider, G. & Wüthrich, K. (1983). *J. Mol. Biol.* **166**, 641–667.

Wagner, B., Kumar, A. & Wüthrich, K. (1981). *Eur. J. Biochem.* **114**, 375–384.

Wagner, G. & Wüthrich, K. (1982). *J. Mol. Biol.* **160**, 343–361.

Wider, G., Macura, S., Kumar, A., Ernst, R. R. & Wüthrich, K. (1984). *J. Magn. Reson.* **56**, 207–234.

Wüthrich, K. (1983). *Biopolymers*, **22**, 131–138.

Wüthrich, K., Wider, G., Wagner, G. & Braun, W. (1982). *J. Mol. Biol.* **155**, 311–319.

Wüthrich, K., Billeter, M. & Braun, W. (1984). *J. Mol. Biol.* **180**, 715–740.

Ziegler, S. M. & Bush, C. A. (1971). *Biochemistry*, **10**, 1330–1335.

Zuiderweg, E. R. P., Kaptein, R. & Wüthrich, K. (1983). *Eur. J. Biochem.* **127**, 279–292.

Edited by M. F. Moody